

Combination Simplex Lattice Design Modelling with Chemometrics Analysis for Optimization Formula Self-Nano Emulsion Loaded Quercetin

Galih Pratiwi^{1,2} , Aninditha Rachmah Ramadhiani¹ , Shaum Shiyani^{3,*} , Lutfi Chabib⁴

¹ Department of Pharmacy, STIKES 'Aisyiyah Palembang, Sumatera Selatan Indonesia, 30152; galihpratiwi@stikes-aisyiyah-palembang.ac.id (G.P.); aninditha.rachmah.ar@gmail.com (A.R.R.);

² Biomaterials and Drug Delivery System (BiDDS) Research Group, STIKES 'Aisyiyah Palembang, Sumatera Selatan Indonesia, 30152

³ Department of Pharmacy, Faculty of Mathematics and Natural Sciences, Universitas Sriwijaya, Indralaya (OI) Sumatera Selatan Indonesia, 30662; shaumshiyani@unsri.ac.id (S.S.);

⁴ Department of Pharmacy, Faculty of Mathematics and Natural Sciences, Universitas Islam Indonesia, Sleman D.I. Yogyakarta, Indonesia; lutfi.chabib@uii.ac.id (L.C.);

* Correspondence: shaumshiyani@unsri.ac.id (S.S.);

Scopus Author ID 57204864081

Received: 12.12.2022; Accepted: 22.02.2023; Published: 2.02.2024

Abstract: Quercetin is formulated as a self-nano emulsion to improve its solubility and bioavailability. This study focuses on optimizing the components of the SSQ-SNE formula using the SLD method and chemometric analysis. SLD is simple, easy to design, and determines the optimal formula of a constant SNE constituent mixture. The concentration of grapeseed oil (%), surfactant tween 80 (%), and co-surfactant PEG 400 (%) were the components that underwent optimization. The selected formulas consist of grape seed oil at 10.0%, tween 80 at 60.0%, and PEG 400 at 30.0%. The selected formula has a droplet size of 14.2 nm, drug load of 48.53 mg/mL, a viscosity of 666.70 mPa.s, emulsification time at aqua dest 3.71 sec, emulsification time at SGF 3.61 sec, emulsification time at SIF 3.30 sec, a viscosity of 370.147 mPa.s, and a drug load of 31.70 mg/mL. Quercetin was successfully formulated into a self-nano emulsion. The model obtained from optimization can be used to predict the character of the optimum formula.

Keywords: quercetin; self-nano emulsifying; simplex lattice design; nanoemulsion; chemometrics.

© 2024 by the authors. This article is an open-access article distributed under the terms and conditions of the Creative Commons Attribution (CC BY) license (<https://creativecommons.org/licenses/by/4.0/>).

1. Introduction

Quercetin has potential pharmacological effects, including antidiabetic [1, 2], anti-inflammatory [3, 4], anticancer [5, 6], and antiviral [7–9]. Quercetin has low bioavailability due to poor solubility. This property causes low absorption in the intestine. Quercetin is included in the biopharmaceutical classification system (BCS) class 2 [10, 11]. Therefore, the development of a delivery system formula can be modified from lipids with self-nano emulsifying (SNE) technology to increase oral bioavailability [10, 12]. The SNE formula is more stable than nano emulsion preparations and is less voluminous than conventional emulsions [13, 14].

SNE is designed in an isotropic liquid system consisting of oil, surfactant, and co-surfactant [15, 16]. The concentration of the composition greatly determines the process of forming an emulsion spontaneously when it meets water. The system formed in SNE is

influenced by the ratio of oil - surfactant, charge, and physicochemical properties [13, 14]. Formula optimization will be carried out using the simplex lattice design (SLD) approach part of the Design of Experiments (DoE). SLD is widely chosen in optimization procedures because it is simple and easy to design and select optimal formulations [17]. SLD determines the optimal formula of a constant amount of SNE constituent mixture. Optimized factors include the concentration of oil, surfactants, and co-surfactants. The nature of each component produces different SNE characteristics. The main parameters as differentiators include emulsification time, viscosity, droplet size, and zeta potential.

2. Materials and Methods

2.1. Chemical materials.

Quercetin was purchased from Sigma-Aldrich. The materials such as grape seed oil, tween 80, propylene glycol, and other materials were purchased from Embacang Multi Sarana (Palembang, Indonesia).

2.2. Optimization design using simplex lattice design (SLD).

Optimization in this formulation uses a design of experiment (DoE) approach. The design and processing of data using Design-Expert software (Stat-Ease Inc., Minneapolis, MN, USA). The design chosen in DoE is part of the simplex lattice design (SLD) of mixture designs. The design uses independent variables grapeseed oil (A; %), Tween 80 (B; %), and PEG 400 (C; %). The responses were selected to be evaluated, namely the transmittance of SNE and nanoemulsion (%), emulsification time (seconds) in three different media, drug load (mg/mL), and viscosity (m.Pa.s). The composition of the mixture of ingredients from each experiment is presented in Table 1.

Table 1. The complete design uses the simplex lattice design (SLD) approach.

Run	Std	A: Grapeseed Oil (%)	B: Tween 80 (%)	C: PEG 400 (%)
1	9	17.5	52.5	30.0
2	5	25.0	45.0	30.0
3	10	20.0	55.0	25.0
4	8	17.5	60.0	22.5
5	6	10.0	60.0	30.0
6	4	25.0	60.0	15.0
7	7	25.0	52.5	22.5
8	1	25.0	52.5	22.5
9	12	17.5	60.0	22.5
10	2	17.5	60.0	22.5
11	11	25.0	52.5	22.5
12	3	17.5	52.5	30.0

2.3. Super saturable quercetin SNE (SSQ-SNE) preparation.

The process began by dissolving quercetin in oil through vortexing for 5 minutes, followed by ultrasonication at room temperature for another 5 minutes. The oil-quercetin solution was then mixed with surfactants and co-surfactants. The mixture formed was stored at 25-30°C for 24 hours [16, 17, 18].

2.4. Percentage of clarity studies (transmittance, %).

The transmittance of the nanoemulsion was determined at a maximum wavelength of 650 nm using a UV-Vis Genesis 10 S spectrophotometer (Thermo Scientific, USA) with <https://biointerfaceresearch.com/>

distilled water as a blank. It gets clearer if the transmittance percentage gets closer to 100%, and it is estimated that the emulsion droplets are nanometers in size.

2.5. Measurement of emulsification time, viscosity, and drug load.

Emulsification times were carried out on quercetin nanoemulsions in aqua dest with three dilution models. A total of 5 mL of media was conditioned above a magnetic stirrer with a speed of 120 rpm at 37°C. SNE of 10 µL, 20 µL, and 50 µL was dripped into each medium quickly until the nanoemulsion was formed. The characterization of the nanoemulsion involved observing the complete dissolution of SSQ-SNE in the medium[18]. The viscosity of SNE-Q is measured using an Oswald viscometer, with the results reported in mPa.s units [10]. The quantity of quercetin loaded in SNE was measured by centrifugation at 3500 rpm for 30 minutes. The precipitate formed is weighed as quercetin which is not loaded into the system.

2.6. Chemometrics analysis

The data obtained were analyzed using chemometrics using the PCA and CA methods. The Minitab 17 series software was utilized to process the PCA-CA method (Minitab, State College, PA, USA). This evaluation stage is not part of optimization and prediction but evaluates the 12 runs and the correlation between responses [18,19].

3. Results and Discussion

3.1. SSQ-SNE formulation.

Quercetin was successfully formulated in the form of an SNE using grapeseed oil as a carrier, tween 80 as a surfactant, and PEG 400 as a co-surfactant. Visualization of 12 experimental runs of SSQ-SNE can be seen in Figure 1.



Figure 1. Visualization of 12 runs of Q-SNE.

Table 2. Visual observation of SSQ-SNE and the formed nanoemulsion.

Run	Visualization SSQ-SNE	Color SSQ-SNE	Precipitate SSQ-SNE	Clarity (% T)	
				SNE	Nanoemulsion
1	No phase separation	Clear yellow	None	66.99	82.05
2	No phase separation	Clear yellow	None	79.12	94.27
3	No phase separation	Clear yellow	None	82.38	91.10
4	No phase separation	Clear yellow	None	72.28	86.82
5	No phase separation	Clear yellow	None	92.98	93.68
6	No phase separation	Clear yellow	None	70.95	89.90
7	No phase separation	Clear yellow	None	81.35	90.19
8	No phase separation	Clear yellow	None	97.85	94.84
9	No phase separation	Clear yellow	None	63.83	80.65
10	No phase separation	Clear yellow	None	66.93	76.77
11	No phase separation	Clear yellow	None	97.70	90.76
12	No phase separation	Clear yellow	None	63.41	83.10

SSQ-SNE shows a yellow-orange color due to the formation of colloidal dispersion. Clarity, measured in percent transmittance, is one of the controls for forming SNE dispersions. Formulas with a %T value of more than 90% indicate that the formula has an apparent visual appearance [1]. With the higher transmittance value, it can be estimated that the nanoemulsion droplets have reached nanometer size. Complete visualization of SSQ-SNE data and the clarity of the nanoemulsion can be seen in Table 2. A total of 10 runs had transmittance values above 90%. Formulas with a %T value of more than 90% indicate that the formula has a clear visual appearance [1]. Clarity, as measured in percent transmittance, is one of the controls for forming SNE dispersions. The clearer or, the greater the transmittance value, it can be estimated that the nanoemulsion droplets have reached nanometer size.

3.2. Optimization of Q-SNE.

The relationship between the variable response (Y) and factor (A, B, C) can be seen in the 3D surface plot (Figure 2). In the transmittance response, each component has a positive influence on the transmittance value. At the same time, the interaction between components can reduce the transmittance value. The interaction between the tween 80 and peg 400 components can increase the emulsification time in aqua dest and SGF media. In the drug load response, the higher the concentration of each component, the higher the drug load. Meanwhile, the interaction between grapeseed oil and peg 400 can reduce drug load. The concentration of each component can reduce the viscosity of SNE.

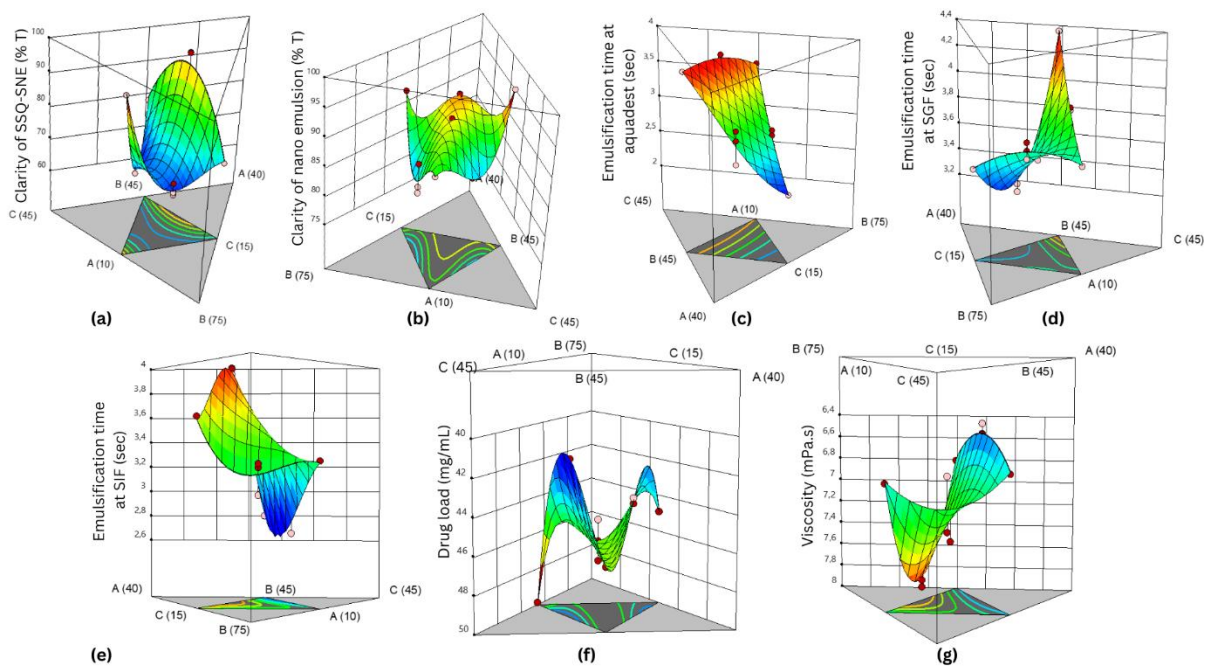


Figure 2. Graph of the 3D model surface plot of the evaluated responses.

Data related to response results from 12 experiments scattered around the diagonal line on the normal plot of residuals (Figure 3). This result indicates that the data is normally distributed and meets the requirements for the analysis of variance (ANOVA) test. Based on statistical analysis, the equation models of the seven responses can be used to predict the optimum mixture of the Q-SNE formulation process. Models of all seven responses showed significant results ($p < 0.05$), and the lack of fit was not significant ($p > 0.05$).

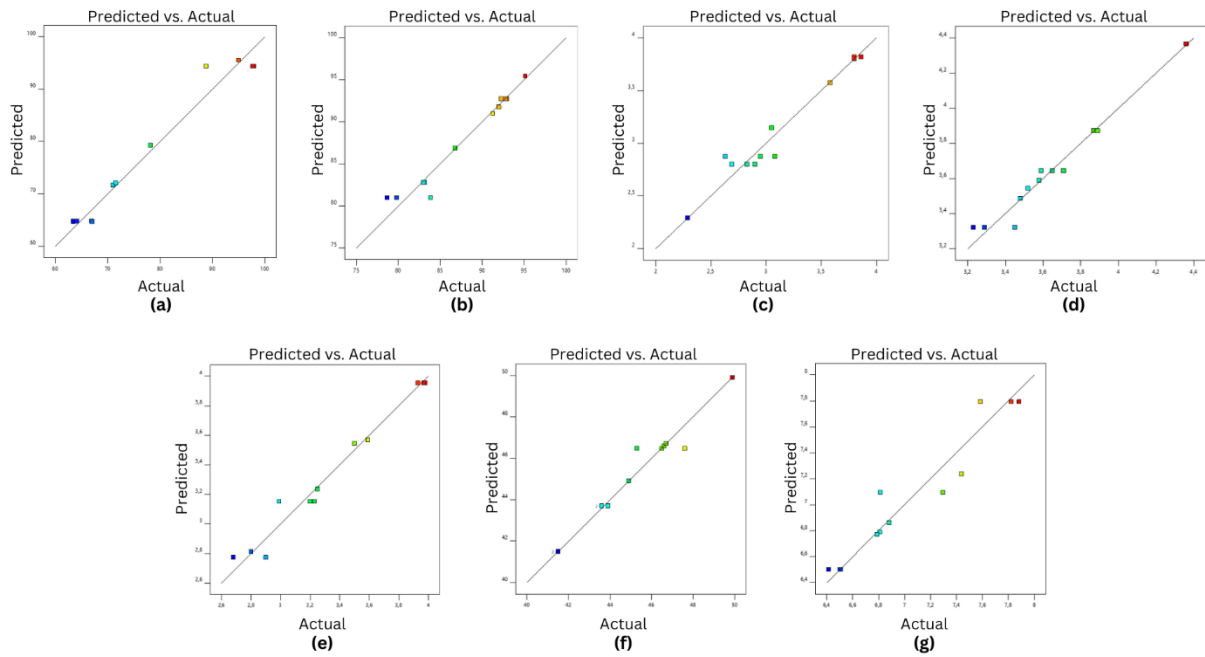


Figure 3. Graph of predicted vs. actual responses.

Table 3. Optimum predicted value, verification range, and verification results.

Parameters	Predicted	Observed	95% CI low	95% CI high	95% TI low	95% TI high
Clarity of SSQ-SNE (% T)	95.50	98.03 ± 0.31	88.30	102.70	74.95	116.05
Clarity of nanoemulsion (% T)	86.87	90.06 ± 0.09	83.51	90.24	77.26	96.48
Emulsification time at aquadest (sec)	3.57	3.71 ± 0.07	3.32	3.82	2.72	4.43
Emulsification time at SGF (sec)	3.59	3.68 ± 0.13	3.47	3.71	3.17	4.01
Emulsification time at SIF (sec)	3.24	3.30 ± 0.14	3.02	3.45	2.62	3.85
Drug load (mg/mL)	49.90	48.5 ± 0.67	48.26	51.53	45.29	54.51
Viscosity (mPa.s)	6.86	6.67 ± 0.25	6.47	7.26	5.72	8.00

The selected oil phase was grape seed oil, tween 80 as the surfactant and PEG-400 as the co-surfactant, with concentrations of 10%, 60%, and 30%, respectively. The desirability value obtained of 0.594 is used as an important indicator in determining the selected formula mix in the SSQ-SNE formulation. In the optimum predicted value, the observed % transmittance of SNEDDS was 98.03 between the range 88.29 - 102.70, and the % transmittance of nanoemulsion was 90.06 in the range 83.50 - 90.23. The observed value of the aqua dest emulsification time was 3.71 from the range of values 3.32 - 3.82, the observed value of the SGF emulsification time was 3.68 between the values of the range 3.46 - 3.71, the value of the SIF emulsification time was obtained 3.30 in the range 3.02 - 3.45. The drug load value obtained was 48.9 in the range of 48.26 - 51.53, and the viscosity value obtained was 6.59 in the range of 6.46 - 7.25. This shows that the results of the optimum prediction meet the verification range (Table 3).

3.3. Characterization and evaluation of selected SSQ-SNE.

3.3.1. Visual appearance.

Visual observations include color, smell, and flow properties. The selected SSQ-SNE formula has a yellowish color, is clear, and has a slightly pungent odor. The addition of surfactants produces a slightly viscous liquid. The resulting yellow color of SNE is influenced by quercetin.

3.3.2. Drug load.

Determination of drug load was carried out using centrifugation at 3500 rpm for 30 minutes; this aims to achieve optimal drug load. The selected SNE showed the presence of a precipitate of 48.53 ± 0.665 (Table 4). The precipitate formed is weighed as the active substance that is not adsorbed into in system [9].

Table 4. Results of verification of selected formulas (n=6).

Parameters	Results
Drug load (mg/mL)	48.53 ± 0.66
Viscosity (mPa.s)	666.70 ± 0.26
Emulsification time at aquadest (sec)	3.71 ± 0.07
Emulsification time at SGF (sec)	3.61 ± 0.12
Emulsification time at SIF (sec)	3.31 ± 0.13

3.3.3. Viscosity.

Viscosity in SNE aims to facilitate the use and formation of nanoemulsions. The low viscosity is affected by the smaller oil globule size [10]. SNE with a lower viscosity emulsifies quickly, while SNE with a high viscosity resembling a gel takes longer to disperse when in contact with water. The SNE viscosity in the selected formulation was 666.70 ± 0.26 mPa.s (Table 4).

3.3.4. Emulsification time.

Analysis of emulsification time is needed to describe the length of time needed for SNE to form nanoemulsions when they meet with liquid in the gastrointestinal tract. The emulsification time requirement for SNE preparations is no more than 5 minutes [9]. The results of measuring the emulsification time response on various media can be seen in Table 6.

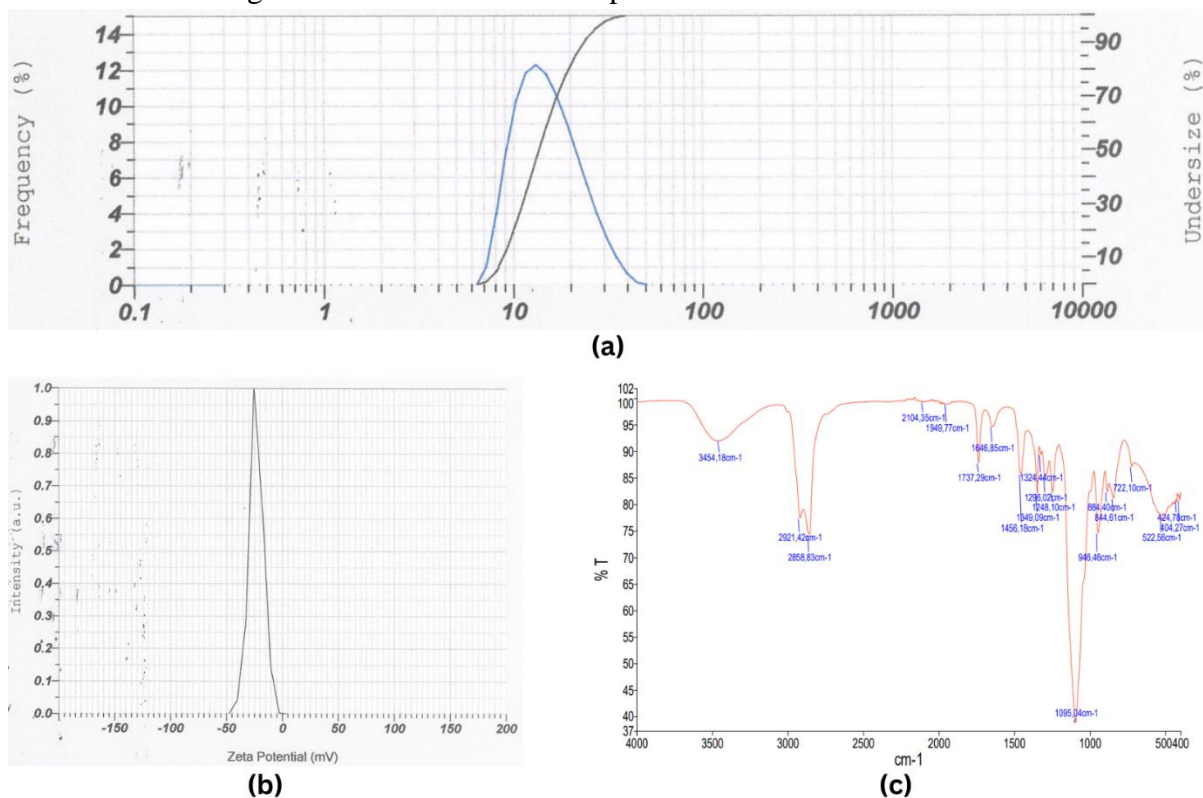


Figure 4. Characteristic of selected formula (a) particle size (nm); (b) zeta potential (mV); (c) FTIR-ATR spectra.

The selected formula shows the emulsification time in aqua dest media is 3.71 ± 0.070 seconds, the gastric fluid media emulsification time (SGF) showed results of 3.68 ± 0.126 , and the intestinal fluid media emulsification time (SIF) was obtained 3.30 ± 0.134 . This shows that the selected formula is a good SNE formula because it gives emulsification results in less than 5 minutes.

Particle size and zeta potential measurements are carried out in the selected formula. The results show that the optimum formula has a particle size of 14.2 d.nm and a zeta potential of -23.77 mV (Figure 4). A value that is further away from the zero number indicates more stability [10]. Small particles with high zeta potential represent high Brownian motion. Therefore, aggregation is not formed to increase stability in the dispersion system [10].

3.4. Multivariate analysis using chemometrics approach.

PCA simplifies variables by reducing data from numerous interconnected variables while preserving the existing information [18- 20]. The CA technique is a method that relies solely on information derived from data, describing relationships between objects or based on their similar characteristics. CA analysis effectively forms and differentiates groups that exhibit the closest relationships, enabling a more detailed and precise presentation of information [21, 22]. The score plot categorizes the samples according to the composition function of the run and the resulting response [13]. The multivariate analysis effectively grouped the runs, placing them at varying distances from one another. The proximity or distance between runs or samples indicates the similarity of their characteristics. A greater distance between the runs signifies a minimal similarity in traits or characteristics [13]. The dendrogram can cluster similar variables together and establish bonds within a group based on the closeness (similarity) value [18]. Figure 5b represents the dendrogram of the characteristic similarity index. Each run is classified based on its level of similarity.

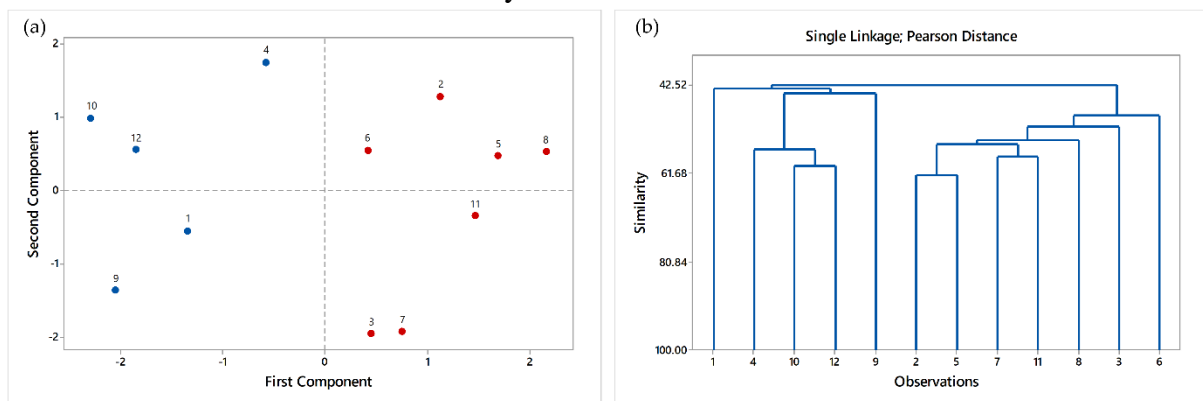


Figure 5. The results of a chemometric analysis using the PCA-CA approach (a) Score plot; (b) Dendrogram.

The loading plot (Figure 6) aims to identify the variable of a sample or formula that contributes the most to the formation of principal component (PC) values. The contribution of the sample variables to the loading plot can be observed through the utilized distance measure. By utilizing the PCA loading plot for data analysis, the angle displayed indicates the correlation between the responses of all formulas. The responses of transmittance for SNE and nanoemulsion, forming an angle that is less than 45° , indicate a positive correlation. Conversely, viscosity and transmittance negatively correlate, forming an angle close to 180° . High viscosity can reduce the percentage of clarity (% T). An angle close to 90° between two vectors indicates no correlation between the responses.

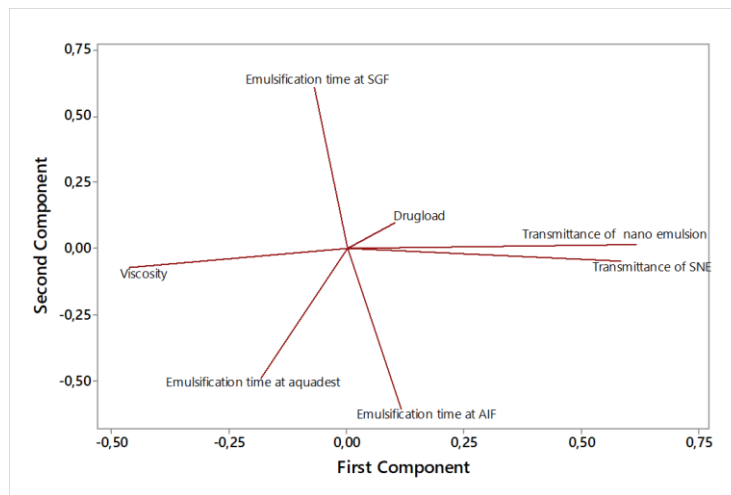


Figure 6. Loading plot The results of a chemometric analysis using the PCA-CA approach.

4. Conclusions

Quercetin was successfully formulated into self-nano emulsion using grape seed oil, tween 80, and peg 400. The model obtained from optimization can be used to predict the character of the optimum formula.

Funding

This study was supported by Direktorat Riset dan Pengabdian Masyarakat Direktorat Jendral Riset dan Pengembangan Kementerian Riset, Teknologi dan Pendidikan Tinggi with contract number 154/E5/PG.02.00.PT/2022; 1384/LL2/PG/2022, in accordance with the Assignment Agreement Letter Implementation of the 2022 Research Program Number: 0257/E5/AK.04/2022

Acknowledgments

The author expresses gratitude for the support provided by the Biomaterials and Drug Delivery System (BiDDS) Research Group and the Department of Pharmacy at STIKES 'Aisyiyah Palembang. Special thanks are extended to the Phytopharmaceutic Research Center (PRC) in the Department of Pharmacy, Faculty of Mathematics and Natural Sciences at Universitas Sriwijaya and the Pharmacy Research Laboratory Universitas Islam Indonesia, Yogyakarta.

Conflicts of Interest

The authors declare no conflict of interest.

References

1. Dhanya, R. Quercetin for managing type 2 diabetes and its complications, an insight into multitarget therapy. *Biomed Pharmacother* **2022**, *146*, 112560, <https://doi.org/10.1016/J.BIOPHA.2021.112560>.
2. Iwara, I.A.; Mboso, E.O.; Eteng, O.E.; Elot, K.N.; Igile, G.O.; Ebong, P.E. *Peristrophe bicalyculata* extract and quercetin ameliorate high fat diet- streptozotocin-induced type ii diabetes in Wistar rats. *Pharmacol Res - Modern Chinese Med* **2022**, *2*, 100060, <https://doi.org/10.1016/J.PRMCM.2022.100060>.
3. He, Z.; Liu, Y.; Wang, H.; Li, P.; Chen, Y.; Wang, C.; Zhou, C.; Song, S.; Chen, S.; Huang, G.; Yang, Z. Dual-grafted dextran based nanomicelles: Higher antioxidant, anti-inflammatory and cellular uptake efficiency for quercetin. *Int J Biol Macromol* **2023**, *224*, 1361-1372, <https://doi.org/10.1016/J.IJBIOMAC.2022.10.222>.

4. Tian, C.; Liu, X.; Chang, Y.; Wang, R.; Lv, T.; Cui, C.; Liu, M. Investigation of the anti-inflammatory and antioxidant activities of luteolin, kaempferol, apigenin and quercetin. *S Afr J Bot* **2021**, *137*, 257–264, <https://doi.org/10.1016/J.SAJB.2020.10.022>.
5. Gökbiçen, S.Ö.; Becer, E.; Vatanserver, H.S. Senescence-mediated anticancer effects of quercetin. *Nutr Res* **2022**, *104*, 82–90, <https://doi.org/10.1016/J.NUTRES.2022.04.007>.
6. Oskooei, F.A.; Mehrzad, J.; Asoodeh, A.; Motavalizadehkakhky, A. Multi-spectroscopic characteristics of olive oil-based Quercetin nanoemulsion (QuNE) interactions with calf thymus DNA and its anticancer activity. *J Mol Liq* **2022**, *367*, 120317, <https://doi.org/10.1016/J.MOLLIQ.2022.120317>.
7. Huang, L.; Li, M.; Wei, H.; Yu, Q.; Huang, S.; Wang, T.; Liu, M.; Li, P. Research on the indirect antiviral function of medicinal plant ingredient quercetin against grouper iridovirus infection. *Fish Shellfish Immunol* **2022**, *124*, 372–379, <https://doi.org/10.1016/J.FSI.2022.04.013>.
8. Manjunath, S.H.; Thimmulappa, R.K. Antiviral, immunomodulatory, and anticoagulant effects of quercetin and its derivatives: Potential role in prevention and management of COVID-19. *J Pharm Anal* **2022**, *12*, 29–34, <https://doi.org/10.1016/J.JPHA.2021.09.009>.
9. Sun, Y.; Li, C.; Li, Z.; Shanguan, A.; Jiang, J.; Zeng, W.; Zhang, S.; He, Q. Quercetin as an antiviral agent inhibits the Pseudorabies virus in vitro and in vivo. *Virus Res* **2021**, *305*, 198556, <https://doi.org/10.1016/J.VIRUSRES.2021.198556>.
10. Pratiwi, G.; Ramadhiani, A.R.; Shiyani, S. Understanding the combination of fractional factorial design and chemometrics analysis for screening super-saturable quercetin-self nano emulsifying components. *Pharmacia* **2022**, *69*, 273–284, <https://doi.org/10.3897/pharmacia.69.e80594>.
11. Rathod, S.; Arya, S.; Kanike, S.; Shah, S.A.; Bahadur, P.; Tiwari, S. Advances on nanoformulation approaches for delivering plant-derived antioxidants: A case of quercetin. *Int J Pharm* **2022**, *625*, 122093, <https://doi.org/10.1016/J.IJPHARM.2022.122093>.
12. Anwer, M.K.; Iqbal, M.; Aldawsari, M.F.; Alalaiwe, A.; Ahmed, M.M.; Muharram, M.M.; Ezzeldin, E.; Mahmoud, M.A.; Imam, F.; Ali, R. Improved antimicrobial activity and oral bioavailability of delafloxacin by self-nanoemulsifying drug delivery system (SNEDDS). *J Drug Delivery Sci Technol* **2021**, *64*, 102572, <https://doi.org/10.1016/j.jddst.2021.102572>.
13. Shiyani, S.; Safitri, I.N.; Nathasia, J.; Fitrotunnisa, L.; Ochita, L.F.; Salsabillah, T.; Pratiwi, G. FTIR spectroscopy combined with chemometrics for evaluation of gambir extract – self nano emulsifying formulation from *Uncaria gambir* Roxb. *Biointerface Res Appl Chem* **2023**, *13*, 153, <https://doi.org/10.33263/BRIAC132.153>.
14. Wahyuni, A.S.; Muhammad, D.; Harlianti, M.S.; Shiyani, S.; Pratiwi, G. Formulation of super saturable-self micro emulsifying loaded *Centella asiatica* L. extract and FTIR-based fingerprinting combined chemometrics analysis. *Asian J Chem* **2022**, *34*, 1477–1482, <https://doi.org/10.14233/ajchem.2022.23530>.
15. Jain, S.; Dongare, K.; Nallamothu, B.; Dora, C.P.; Kushwah, V.; Katiyar, S.S.; Sharma, R. Enhanced stability and oral bioavailability of erlotinib by solid self nano emulsifying drug delivery systems. *Int J Pharm* **2022**, *622*, 121852, <https://doi.org/10.1016/J.IJPHARM.2022.121852>.
16. Jindal, A.; Kumar, A. Physical characterization of clove oil based self Nano-emulsifying formulations of cefpodoxime proxetil: Assessment of dissolution rate, antioxidant & antibacterial activity. *OpenNano* **2022**, *8*, 100087, <https://doi.org/10.1016/J.ONANO.2022.100087>.
17. Pratiwi, G.; Martien, R.; Murwanti, R. Chitosan nanoparticle as a delivery system for polyphenols from meniran extract (*Phyllanthus niruri* L.): Formulation, optimization, and immunomodulatory activity. *Int J Appl Pharm* **2019**, *11*, 50–58, <https://doi.org/10.22159/ijap.2019v11i2.29999>.
18. Shiyani, S.; Zubaidah; Pratiwi, G. Chemometric Approach to Assess Response Correlation and its Classification in simplex centroid design for Pre-Optimization stage of Catechin-SNEDDS. *Res J Pharm Technol* **2021**, *14(11)*, 5863–70, <https://doi.org/10.52711/0974-360X.2021.01020>.
19. Kartini K.; Putri, L.A.D; Hadiyat, M.A. FTIR-based fingerprinting and discriminant analysis of *Apium graveolens* from different locations. *J Appl Pharm Sci* **2020**, *10(12)*, 62–7. <http://dx.doi.org/10.7324/JAPS.2020.101208>
20. Ariyanthini, K.S; Angelina, E.; Andina, N.K.D.P; Wijaya, H.; Wiratama, I.P.R.K.P.; Naripradnya, P.S.; Putra, I.G.A.N.D.; Setyawan, E.I. Implementation of Principal Component Analysis-Cluster Analysis on the Extraction of Green Tea Leaf (*Camellia sinensis* (L.) Kuntze). *Biointerface Res App Chem* **2023**, *13(4)*, 335. <https://doi.org/10.33263/BRIAC134.335>

21. Nainggolan, R.; Eviyanti, P. The Cluster Analysis of Online Shop Product Reviews Using K-Means Clustering. *Data Sci J Comput Appl Informatics* **2020**, *4*(2),111–21. <http://dx.doi.org/10.29138/ijebd.v3i02.977>
22. Crase, S.; Hall, B.; Thennadil, S.N. Cluster Analysis for IR and NIR Spectroscopy: Current Practices to Future Perspectives. *Computers, Materials & Continua* **2021**, *69*(2), 1945-1965. <https://doi.org/10.32604/cmc.2021.018517>